

## **An Accessible NDVI Classification Tool for Urban and Suburban Vegetation Change Analysis**

Aurash Khawarзад, PhD student

The Graduate Center at the City University of New York, Earth and Environmental Sciences dept

[akhawarзад@gradcenter.cuny.edu](mailto:akhawarзад@gradcenter.cuny.edu)

ORCID: 0009-0005-9428-8467

January 29, 2026

### **Abstract**

This paper presents a web-based research method for studying changes in vegetation in urban and suburban contexts between 2018 and 2024. The system uses the Normalized Difference Vegetation Index (NDVI) to analyze imagery for each period and classify land surface types. After classification, correlation and regression analysis are applied to explain connections between urbanization and vegetation change over time. Two case studies are included to demonstrate the method's validity: suburban Warrenton, Virginia and urban Portland, Oregon, which have contrasting physical characteristics and land use policies. By providing workflow documentation and using open source technology, this method democratizes land classification analysis for researchers in planning, conservation, and related fields. Potential improvements for this tool include: 1-higher resolution imagery; 2-conducting field research to verify results and build regional models; and 3-improve NDVI application for broader land classification results. The research method is available for public use at: <https://terrestrialresearch.com/machinelearning/landclass2>.

**Keywords:** open source GIS, remote sensing tools, vegetation growth analysis, land use/land cover change (LULCC) methodology, accessible research tools

### **Research application website**

<https://terrestrialresearch.com/machinelearning/landclass2>

### **Github repository**

<https://github.com/aurashak/ndvilandclass>

## **1. Introduction**

This paper proposes a method for using open satellite data and GIS programming to measure changes in vegetation in the urban and suburban context between 2018 and 2024. This method provides an accessible land classification and statistical analysis tool for researchers, professionals, and community members, alike. By providing documentation on building the web-based tool for land classification, and the equations for analyzing the land

classification data, this method can be adapted and applied in a variety of social and geographic contexts. 43  
44

The main processing tool in this method, the NDVI, is a well-established remote sensing tool that observes near-infrared (NIR) and red wavelengths that are reflected by all surface types of the earth (Tucker, 1979). The NDVI has been proven capable of identifying most the earth's surface types, given they each absorb and reflect a distinct type of infrared light (Goward et al., 1991). But it has proven most applicable in identifying the growth and health of plant life (Pettorelli et al., 2005). 46  
47  
48  
49  
50  
51

Underlying this method is a web-based architecture that uses HTML, JavaScript, and Python geospatial analysis. These systems communicate with the European Space Agency (ESA) data portal, analyze satellite data, and present analyzed data for the public (Drusch et al., 2012). Using a Leaflet.js mapping browser, the user navigates to an area of the globe and captures a screenshot of the area for the years 2018 and 2024. A Python script then communicated with ESA data using API, where the NDVI algorithm is applied to each pixel captured. The script then determines the percentage of change in land cover for each image. Land cover types that are specifically measured include water, bare paved surface, sparse vegetation, moderate vegetation, and dense vegetation. 52  
53  
54  
55  
56  
57  
58  
59  
60  
61

Two applications of this method are included below, one for suburban Warrenton, Virginia and one for urban Portland, Oregon. The locations were chosen for their climates that both support wide growth of vegetation cover, and for their contrasting land use policies, with Warrenton developing sprawling housing subdivisions, and Portland densifying and restricting sprawl. After running the land classification analysis for each location during each time period, a correlation analysis and regression analysis was applied to determine if there is a relationship between the changes or if they operate independently of each other. Using this method, it was determined that there is a weak positive relationship between suburban development and loss of vegetation in Warrenton, while there is also a weak positive relationship between increased urban development and growth of additional vegetation in Portland. 62  
63  
64  
65  
66  
67  
68  
69  
70  
71  
72  
73

While the analysis of Warrenton and Portland supports the hypothesis that suburban sprawl contributes to loss of vegetation when compared to urban densification, there are several limitations to this study including the satellite hardware and programming software. Satellites being launched soon will also provide more accurate and robust capabilities for land classification approaches like this, as long as data are made publicly accessible (NASA Jet Propulsion Laboratory, 2023). 74  
75  
76  
77  
78  
79  
80

The methodology is designed for researchers working in policy, planning, engineering, design, conservation, and related disciplines. Quantifying the changes in land cover types 81  
82  
83

can provide a metric for analyzing the impacts of urban plans and the impacts of development (Lunetta et al., 2006). This information can support further planning and design interventions for the preservation of vegetated areas and to mitigate the social impacts of areas experiencing loss in vegetation. This research is an example of a complete workflow for socio-environmental analysis that was not previously available to the public.

## 1.1 Research Objectives

- Methodological framework: Provide detailed documentation developing a land classification method using open data that is designed to study urban and suburban contexts. The utilization of open data and open source technology makes this approach replicable and accessible.
- Example analysis: Conduct two example analyses of the urban and suburban context to demonstrate the research method and include the results.
- Challenges: Using open data and open source technology creates several challenges for obtaining accurate results and maintaining systems long-term. This paper documents challenges such as inconsistency in access to quality data, both in terms of time period available and resolution of imagery.
- Opportunities: Satellite technology will be deployed soon that will make much more robust and detailed analysis possible. Below are opportunities for those technological and programmatic updates to benefit publicly available land classification systems, like this one.

## 2. Methods

### 2.1. Web Application Infrastructure

#### 2.1.1. Frontend Design

This system is divided between the frontend (HTML and JavaScript), where the viewer can select the location they want to apply the research method and view the maps, text, charts and other results; and the backend (Python), where scripts are executed that retrieve data from the web and apply the NDVI algorithm. Leaflet.js is used as open source mapping framework for displaying satellite data collected by Sentinel-2 (Agafonkin, 2011).

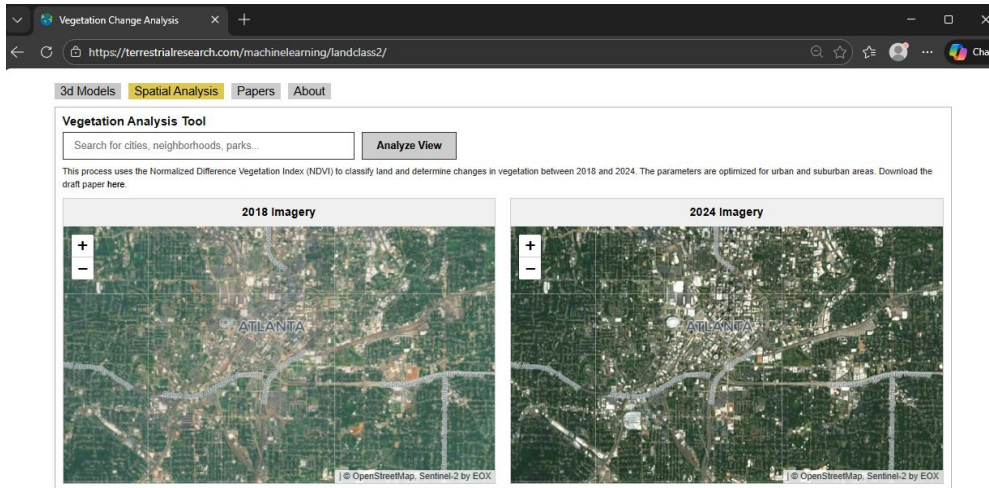


Figure 1: Land Classification Web Application.

## 2.2.2. Backend Computation

The Python script retrieves data from the Copernicus data hub via API, then accesses the Pillow, NumPy, Matplotlib, and SciPy libraries to conduct statistical analysis and produce data visualizations for the NDVI results (Harris et al., 2020; Hunter, 2007; Virtanen et al., 2020). These libraries provide the capabilities for processing satellite data, including massive tables and arrays containing billions of data points for geographic coordinates, color, height, and other data used in LULLC.

## 2.2.3. LLM-Assisted Coding

The open source Large Language Model (LLM) qwen3-coder was used to assist with coding and debugging for Python and JavaScript. Server infrastructure, online interface, mapping framework (Leaflet, QGIS, etc), API connectivity (Copernicus), and statistical analysis methods were developed by the author, while LLMs assisted with accessing open source coding language and debugging.

## 2.2. Satellite Imagery Limitations

### 2.2.1. Sentinel-2 Satellite Constellation

The ESA's Sentinel-2 constellation provides one of the most robust geospatial datasets available to the public (Drusch et al., 2012). Originally composed of two satellites, Sentinel-2A and 2B, a third satellite, Sentinel-2C, was launched in September 2024. These satellites synchronization reduces the global revisit time from five days to just 2–3 days, which is critical for mitigating cloud cover interference and capturing narrow windows of "peak greenness" for NDVI calculations (Verbesselt et al., 2010).

### 2.2.2. Resolution and Temporal Limitations

Sentinel-2 collects imagery data at a resolution of 10m per pixel, while data collected by commercial providers like Maxar (WorldView) or Planet (SkySat), offer Very High

116

117

118

119

120

121

122

123

124

125

126

127

128

129

130

131

132

133

134

135

136

137

138

139

140

141

142

143

144

145

Resolution (VHR) imagery that reaches up to 30 cm per pixel (EOPortal, 2025) (NASA 146  
CSDA, 2025; Maxar Technologies, 2025). State agencies and subscription services, such as 147  
NASA's Commercial Smallsat Data Acquisition (CSDA) Program and Google Earth Pro, 148  
respectively, offer access to high-resolution data through private contracts and consumer 149  
subscriptions. Higher resolution imagery can provide more data for the algorithm and thus 150  
classify greater quantities of land and classify it with greater detail, vs lower resolution 151  
imagery. And unlike Sentinel-2's fixed orbit, these satellites have greater flexibility in what 152  
they observe, rather than waiting for an orbital pass. Sentinel-2 has other disadvantages in 153  
sensor technology and positioning, making it susceptible to cloud cover and unable to ac- 154  
curately classify certain land types. 155

The timeframe of 2018 to 2024 was chosen for this research because that is the oldest and 157  
most recent data made publicly and freely available by the Copernicus program at con- 158  
sistent 10-meter resolution (Drusch et al., 2012; ESA, 2024). Older Sentinel-2 data is availa- 159  
ble dating back to 2015, but early programs had reduced coverage and higher cloud rates 160  
before the full two-satellite constellation was launched (Verbesselt et al., 2010). While some 161  
historical imagery is offered freely through platforms like Google Earth, it is not accessible 162  
via Application Programming Interface (API) using open data standards and thus presents 163  
significant technical challenges for creating publicly available, automated research tools 164  
like the method presented here (Google Earth, 2025). 165

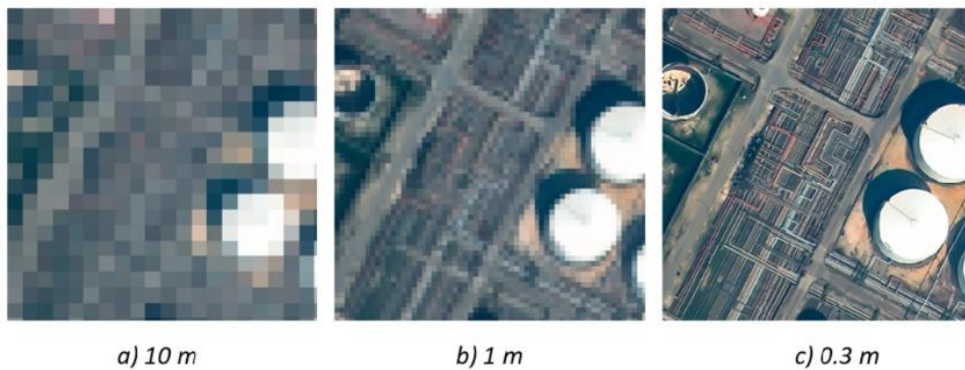


Figure 2: Imagery comparison at the 10m, 1m, and 30cm resolution (Romaniuk, 2023). 167

This method operates at the 10m scale. 168

## 2.3. Normalized Difference Vegetation Index (NDVI) and Land Classification 170

### 2.3.1. NDVI Formula and Application 171

The near infrared (NIR) data that is analyzed by the NDVI is captured by multispectral 172  
cameras on the Sentinel-2 satellites. This web application allows the viewer to select a 173  
512px by 512px area of the earth and to analyze each pixel in that section for near infrared 174  
and red band light using the formula (Tucker, 1979): 175

$$NDVI = \frac{(NIR - Red)}{(NIR + Red)} \quad 176$$

179  
180  
181  
182  
183  
184  
185  
186

### 2.3.2. Classification Thresholds

The formula calculates a value between -1 to +1 for each pixel. Higher values within that range represent vegetation, while low and negative values typically represent water, bare soil, and paved surfaces (Pettorelli et al., 2005). In this method, the Python script converts the NDVI value to a color range for visualization on the map. The values are converted into these categories and colors:

| NDVI Range  | Description         | Color Code   |
|-------------|---------------------|--------------|
| < -0.1      | Water               | Blue         |
| -0.1 to 0.2 | Bare/Urban          | Gray         |
| 0.2 to 0.35 | Sparse Vegetation   | Light Yellow |
| 0.35 to 0.5 | Moderate Vegetation | Light Green  |
| ≥ 0.5       | Dense Vegetation    | Dark Green   |

187  
188  
189  
190  
191  
192  
193  
194  
195  
196  
197  
198  
199  
200  
201  
202

### 2.3.3. Full Spectrum of Land Cover Classification

This application does not capture the full categories that are detectable by the NDVI. This tool excludes land types that are not typically found in urban or suburban contexts, such as rainforest, agriculture, deep water, and ice. Excluding these surfaces has the potential to improve the accuracy for remaining surface types. However, it also makes this method and online application unapplicable to geographic areas like the Amazon that exist in the higher range of vegetation density, the Arctic tundra and other ice or sand covered terrains with little to vegetation, the earth's oceans, seas, and other deep bodies of water, among a few others. This algorithm is not designed to capture phases of the agricultural process, which is possible with the NDVI index, but rather groups agricultural land with the bare soil category. Modification of the NDVI index to focus on urban and suburban contexts is an example of tailoring online applications for professional fields, like urban planning and design, compared to other fields that may be analyzing excluded terrains such as vast forests or aquatic habitats.

The standard multispectral data that is captured by Sentinel-2 consists of 12–13 bands, which is enough data to determine if land is light to dense vegetation (Drusch et al., 2012). Data collection on forthcoming satellites will be hyperspectral and will include 100 to 200+ very narrow bands, which is enough detail to determine what type of trees and miscellaneous vegetation are captured in satellite imagery and even if they have specific nutrient deficiencies, among other detailed measurements (NASA Jet Propulsion Laboratory, 2023). Another method of improving these results is to combine field data with Machine Learning

programs, to localized environments for the application. This would allow researchers to account for local and regional contexts like weather patterns, vegetation types, pavement types, and more metadata about the location. "Training" this model using field data and machine learning would make the results more relevant and reliable.

#### 2.3.4. Scale of Imagery

The NDVI is best applied between specific elevations, based on the capability of the sensor technology capturing imagery data. For this application, the Leaflet.js map applies a zoom lock, so the camera can only view land between an elevation of roughly 1,800m and 2,200m (5,900ft and 7,200ft). This altitude for the camera places the maps at a roughly 1:15,000 scale and 1:18,000 scale, respectively. Zooming out further to a higher elevation and larger map scale in an application like this is not ideal because the capture area will include a higher mixture of pixels, including shadows, clouds, and greater diversity of surface types, will confuse the program and reduce its accuracy.

#### 2.4. Statistical Analysis

As stated previously, the NDVI uses near infrared imagery data captured from satellites to create a value between -1 to 1 that it assigns to each pixel of the area being analyzed by the application, with the lower end of the spectrum representing unvegetated areas and the higher end representing vegetated areas (Tucker, 1979). The statistical analysis portion of this method compares the difference in value for each pixel between the imagery captured in 2018 and 2024 (Singh, 1989).

##### 2.4.1. Change to Urban and NDVI Change

In this model, the independent variable is the "urban\_gain" value in the formula below, which is a 0 or 1 classification indicating whether a pixel changed to built environment. In Python the formula to determine this value is:

```
urban_gain = ((classes_2018 != 1) & (classes_2024 == 1)).astype(int)
```

The dependent variable is the difference in vegetation, measured as the continuous numerical change in NDVI values for that same pixel between the satellite images. The Python code used in this project to determine the change in NDVI value for each pixel is:

```
ndvi_change = ndvi_2024 - ndvi_2018
```

Using mathematical notation:

$$\Delta NDVI_i = NDVI_{2024,i} - NDVI_{2018,i}$$

Where:

$\Delta\text{NDVI}_i$  = change in NDVI for pixel i 251  
 $\text{NDVI}_{2024,i}$  = NDVI value for pixel i in 2024 252  
 $\text{NDVI}_{2018,i}$  = NDVI value for pixel i in 2018 253

By isolating these variables, the analysis can test the hypothesis that urban development and loss of vegetation are connected. 255  
 256

#### 2.4.2. Pearson's r correlation coefficient 258

Once it is determined which pixels have transitioned from vegetated to paved/bare classification (urban\_gain) and the NDVI change for each pixel (ndvi\_change), a correlation analysis is done using the Pearson's r technique (Virtanen et al., 2020). This correlation analysis establishes if there is a link between urbanization and the decrease vegetation. Determining correlation is important because while simple land classification can show if vegetation is being lost, it does not mathematically prove the relationship to development. Pearson's r measures the relationship between urbanization and vegetation. 259  
 260  
 261  
 262  
 263  
 264  
 265

The formula for determining correlation (Pearson's r) is: 267

$$r = \frac{\Sigma[(x_i - \bar{x})(y_i - \bar{y})]}{\sqrt{\Sigma(x_i - \bar{x})^2 \cdot \Sigma(y_i - \bar{y})^2}}$$

Where: 270

$x_i$  = UrbanGain<sub>i</sub> 271  
 $y_i$  =  $\Delta\text{NDVI}_i$  272  
 $\bar{x}$  = mean of UrbanGain 273  
 $\bar{y}$  = mean of  $\Delta\text{NDVI}$  274

This Python code determines the link between urban\_gain (x) and the ndvi\_change (y): 276

```
r_value, p_value = stats.pearsonr(urban_gain_valid, ndvi_change_valid)
```

The correlation coefficient (r) from that formula ranges from -1 to +1. In this study, a value near -1 indicates a strong inverse relationship, confirming that urban expansion is directly tied to vegetation loss. Conversely, a value of 0 would indicate no linear relationship between the two variables. A value of 1 would mean a positive correlation of both urban growth and vegetation growth. The p-value (p\_value), with a significance level of < 0.05, ensures the correlation is reliable (Virtanen et al., 2020). 280  
 281  
 282  
 283  
 284  
 285

#### 2.4.3. Linear Regression 287

After establishing correlation through Pearson's r, a linear regression model is applied to quantify the level of NDVI change associated with urbanization. This regression measures 288  
 289

exactly how much vegetation loss occurs when a pixel transitions to urban development (Virtanen et al., 2020). The Python implementation uses:

```
slope, intercept, r_val, p_val, std_err = stats.linregress(urban_gain_valid,  
ndvi_change_valid)
```

The regression equation takes the form:

$$\text{NDVI Change} = \beta \times (\text{Urban Gain}) + \alpha$$

Where:

$\beta$  = slope (regression coefficient)

$\alpha$  = intercept

The slope ( $\beta$ ) and intercept ( $\alpha$ ) are the two key parameters that define the linear relationship between urbanization and NDVI change. A negative slope shows that urbanization is causing loss of vegetation. The intercept represents the expected NDVI change for non-urban pixels (where urban\_gain = 0), establishing a baseline trend that accounts for natural environmental variations unrelated to urbanization, such as changes in climate.

#### 2.4.4. R<sup>2</sup> Coefficient of Determination

The coefficient of determination (R<sup>2</sup>) measures how well the regression model explains the observed data (Virtanen et al., 2020). It is calculated as the square of the correlation coefficient (r) obtained from the Pearson's r analysis in the previous step. R<sup>2</sup> indicates the proportion of NDVI variance explained by development. A higher R<sup>2</sup> value means that a greater percentage of observed vegetation change can be attributed specifically to urban expansion, while the remaining variance results from other factors such as climate or land management practices. The formula for this calculation is:

$$R^2 = r^2$$

R<sup>2</sup> indicates the proportion of NDVI variance explained by development. A higher R<sup>2</sup> value means that a greater percentage of observed vegetation change can be attributed specifically to urban expansion.

The p-value from the regression analysis, similar to the p-value from the correlation test, confirms the statistical significance of the relationship.

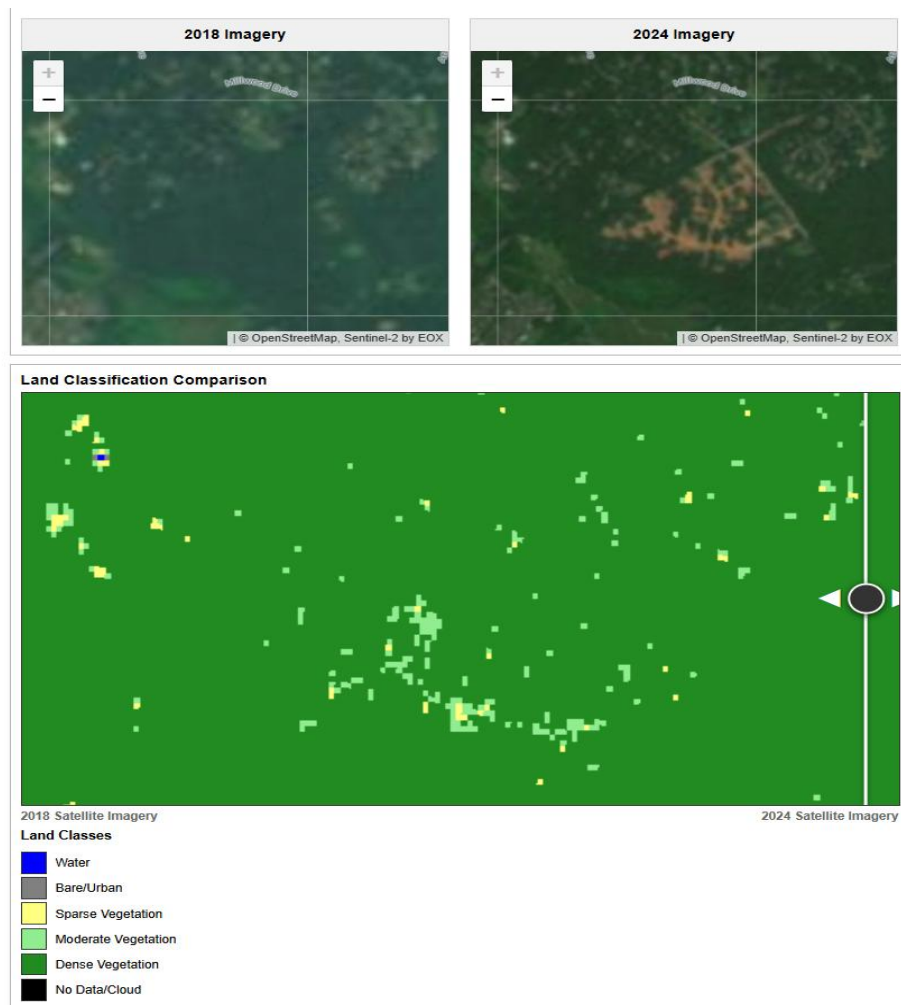
### 3. Results

This paper includes analysis of two distinct regions to demonstrate performance across different contexts: a dense urban area growing through densification rather than sprawl, and a rural area experiencing rapid suburban style sprawl, with those areas being Portland,

Oregon; and Warrenton, Virginia, respectively. These locations were selected to represent 331  
contrasting approaches to urban growth and land use planning in the United States. These 332  
locations were also chosen for their vegetated conditions, which are easily recognizable by 333  
the Sentinel-2 MSI, as opposed to surfaces that may have snow or sand, which can require 334  
adjustment of the algorithm (Verbesselt et al., 2010). 335

### 3.1. Study Area 1: Warrenton - Exurban Northern Virginia 336

The municipality of Warrenton is located approximately 50 miles west of central Washing- 337  
ton D.C., within commuting distance of the metropolitan region's outer suburbs and em- 338  
ployment centers. The analyzed area covers approximately 0.64 square miles (1.65 square 339  
kilometers) in the 512 pixel by 512 pixel grid (for a total of 262,144 pixels analyzed). This 340  
specific section was selected because there are clear signs of land development occurring 341  
between the 2018 and 2024 capture periods of satellite imagery. It's clear that vegetation 342  
has been removed in a wide swath of territory. The suburban and exurban areas of Virginia 343  
were selected because they rank among the fastest growing suburbs in the United States 344  
for the study period - having added 90,000 residents between 2023-2024 alone (Wilder and 345  
Mackun, 2025). 346



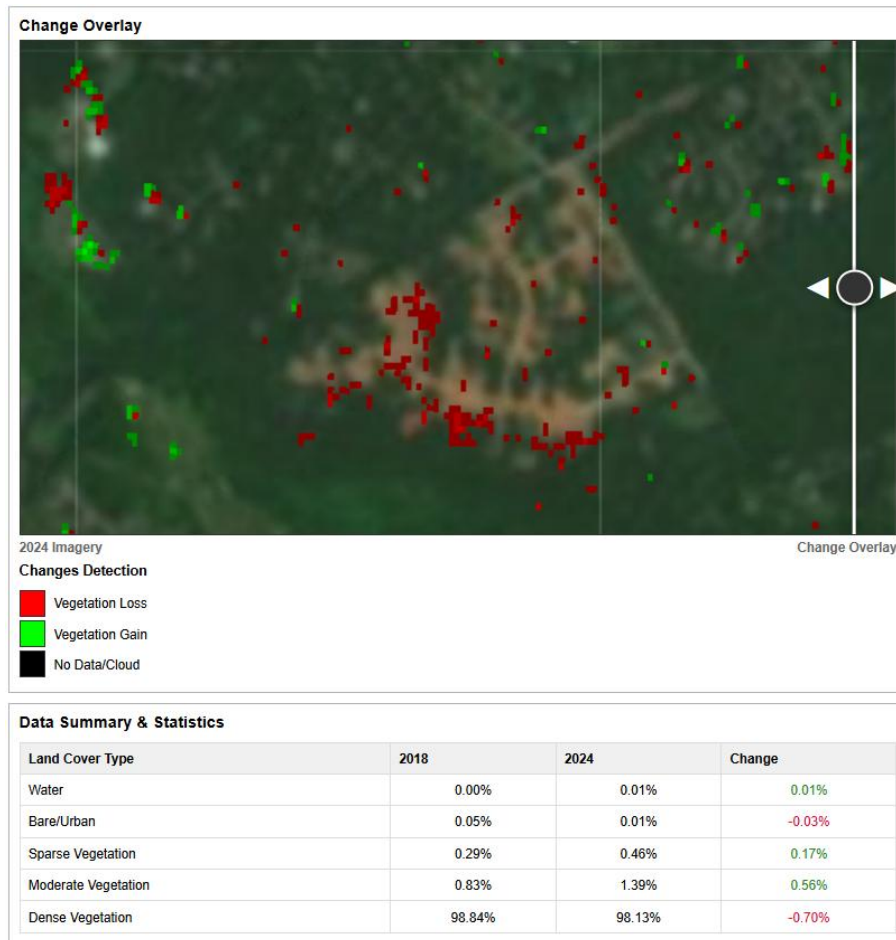


Figure 3: Warrenton, Virginia analysis.

Location analyzed: 38.719° to 38.730° N and longitudes 77.773° to 77.755° W.

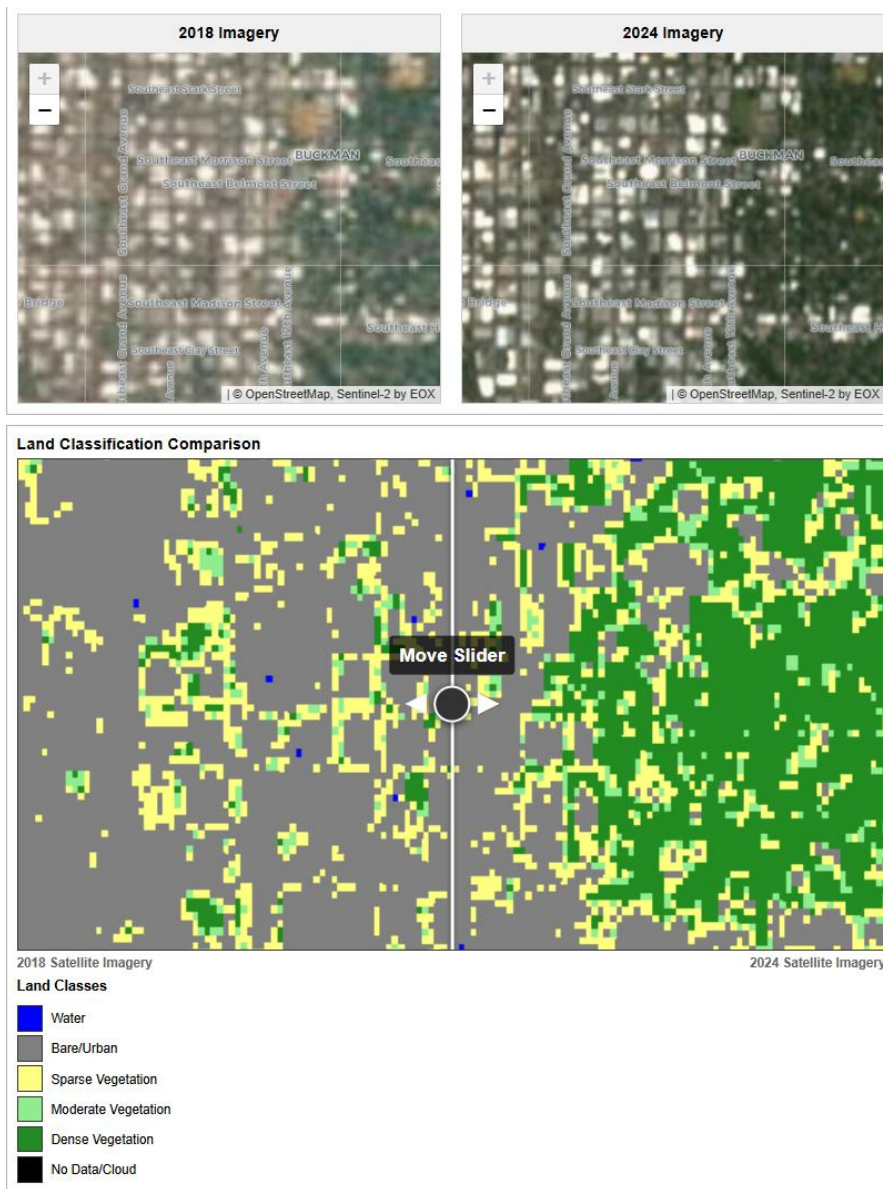
The analysis does not directly classify new development but does show a notable decline in overall vegetation (NDVI). Mean NDVI dropped from 0.934 in 2018 to 0.843 in 2024, representing a decrease of -0.090 (approximately 9.7%). Even with the decline, the region remained forested, with dense vegetation comprising over 98% of land cover in both time periods. This reduction can be seen in the imagery where vegetation has been removed - although other areas may have grown more, thus compensating for the removal. The NDVI change range of -0.714 to +0.575 indicates substantial localized variation, with some areas experiencing severe vegetation loss while others showed improvement. It's also clear from the red pixel visualization that the algorithm does not identify all pixels that have lost vegetation but does show general trends.

The statistical relationship between development and vegetation change in the Warrenton analysis reveals a small negative correlation ( $r = -0.005$ ,  $R^2 = 0.0\%$ ). The regression model shows a negative slope ( $\beta = -1.081$ ), indicating that areas experiencing development averaged NDVI losses of -0.736 compared to gains of +0.344 in non-developed areas. The

changes in land classification show a minimal net change, over 90% of pixels remained in the same class, 4.5% gained vegetation, and 3.8% lost vegetation (Singh, 1989).

### 3.2. Study Area 2: Portland - Urban Core

The Portland metropolitan area was selected as a contrasting area due to its reputation for progressive land use planning policies, including an urban growth boundary (UGB) established in 1979, transit-oriented development (TOD) initiatives, and lauded sustainability programs (Metro, 2023; Abbott, 2001). The analyzed area covers approximately 1.4 square miles (3.6 square kilometers) or 262,144 pixels analyzed. This specific section was selected to examine vegetation dynamics in an urban core, where growth is occurring through densification and infill development rather than outward sprawl.



381

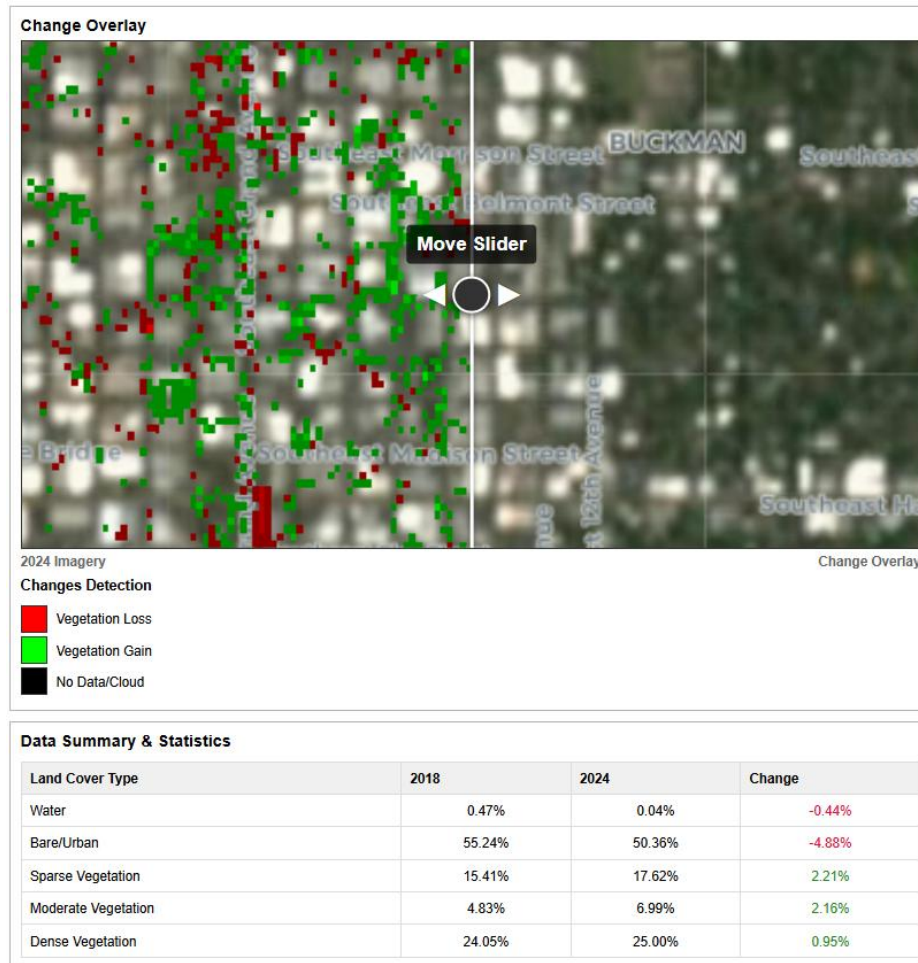


Figure 4: Portland, Oregon analysis

Location: latitudes 45.505° to 45.526° N and longitudes 122.667° to 122.631° W.

The statistical relationship between development and vegetation change in this part of Portland reveals a weak positive correlation ( $r = 0.095$ ,  $R^2 = 0.9\%$ ). The regression model shows a positive slope ( $\beta = 9.500$ ), indicating that areas experiencing development averaged NDVI gains of +9.533 compared to gains of +0.033 in non-developed areas. With 10,363 pixels (3.95%) classified as experiencing development, or urban gain, which are areas that transitioned to paved or bare surfaces, the urban expansion represents approximately 4% of the total study area. The changes in land classification shows a counter-intuitive change: bare/urban surfaces decreased from 55.2% to 50.4% (-4.8%), while vegetation coverage increased across all categories (sparse +2.2%, moderate +2.2%, dense +0.9%). When combined with knowledge that the population of the city grew during this period, this pattern suggests greening within the urban fabric rather than vegetation loss from development.

### 3.3. Data Verification

To assess the accuracy of this method, these results were compared against other land classification systems that apply the NDVI formula. However, several limitations emerged in finding similar datasets and approaches for validation.

The National Land Cover Database (NLCD), which is offered by the USGS, is considered the most extensive and accurate land classification system for the United States (Homer et al., 2020). However, the NLCD has limitations including:

- Temporal mismatch: The most recent publicly available NLCD is from 2021, pre-dating this study's 2024 analysis period by three years.
- Resolution difference: NLCD's 30m resolution is lower than Sentinel-2's 10m, making comparison imprecise

The Copernicus Global Land Cover is another extensive land classification model. But while it is updated and made publicly available every year, matching the Sentinel-2 data, it collects data at the 100m resolution, which is much lower than Sentinel-2, making comparison impossible.

The most decisive way to verify the data being analyzed by this model, or any land classification program, is verification via direct observation. This would be physically visiting specific locations to verify the land cover type. This ground-truthing would verify the existing approach, while providing valuable training data that could support regional approaches for doing land classification analysis. Field observations were beyond the scope of this study but could support future work.

## 4. Discussion

### 4.1. Potential Applications

With there being a historical record of quality satellite data now available to the public, it is possible to determine the efficacy of developing policies and to plan future actions. Potential applications for such land classification tools include any discipline measuring the health of the environment, including how it relates to the growth of human settlement. Specific opportunities include, but are not limited to:

- Monitoring street tree planting programs: check if developers have implemented planting programs; determine if public agencies are meeting planting targets and conducting maintenance.
- Urban forest management: Track canopy loss due to urbanization, mining and extraction, disease, etc (Lunetta et al., 2006).
- Track climate patterns: Determine impacts from long-term climate change or extreme events, including ecosystem health, land erosion and more (Verbesselt et al., 2010).

- Urban heat island mitigation: Identify areas with lack of vegetation and tree cover as potential urban heat islands; Mark UHI zones for future planning and research, including cooling centers, adding vegetation, building renovation, and more.
- Environmental impact assessments: Development projects increasingly require mitigation of ecosystem impacts.
- Baseline vegetation mapping: Establish pre-development conditions that can be used to determine general trends and impacts from development projects (Pet-torelli et al., 2005).
- Archeology and cultural studies: Showing various levels and types of vegetation can indicate recent and historic developments, such as built structures, agriculture, and more.

## 4.2. Future Enhancements

The methodology presented in this paper is proof of concept. However, several enhancements can be made to improve accuracy and range.

## 4.3. Ground Reference Data

Building a reference model for this application would improve accuracy by accounting for regional and local differences between urban and suburban contexts. By having researchers create a catalog of plant types and surface types for a particular area and by identifying the infrared signature of each plant and surface type for that area, the NDVI calculation process can be read with greater levels of accuracy and confidence. The categories will not only be “sparse” or “moderate” vegetation, for example, but specific plant types and their health could be identified. Building a ground model reference data set would allow versions of this tool to be built for distinct geographies and research disciplines.

### 4.2.2. Higher Resolution Imagery

Higher resolution satellite imagery is available from commercial providers like Planet or Maxar and would enable analysis of a wider band of spectral light. This would allow identification of plant types, small green spaces such as pocket parks, and home gardens, and street trees, which may not be picked up with current systems (Drusch et al., 2012). While the instruments on the Sentinel satellites capture data at a resolution of 10 meters per pixel, other satellites exist now that can capture data at up to 30 centimeters per pixel. In the future, higher resolution data will become available and existing high-resolution data has the potential to be freed from behind the paywall. Higher resolution imagery benefits infrared analysis, just as it makes RGB images of greater quality.

### 4.2.3. Hyperspectral Sensors

In 2024 the ESA launched the Sentinel-2C satellite to join the 2A and 2B constellation. Data from that satellite was not available for this study, but it will soon provide additional coverage that can improve the consistency of existing data. However, upcoming missions such

as ESA’s CHIME (Copernicus Hyperspectral Imaging Mission for the Environment) and NASA’s Surface Biology and Geology (SBG) mission, will include hyperspectral sensors capturing 100 to 200+ narrow spectral bands, compared to the 13 multispectral bands provided Sentinel satellites, as detailed above (NASA Jet Propulsion Laboratory, 2023). This dramatically increased resolution enables highly detailed vegetation identification, allowing researchers to distinguish species, identify invasive vegetation, and map ecosystems.

These opportunities, and expected increases in computing power, will greatly improve the capabilities of satellite-based land classification systems.

## 5. Conclusion

This paper demonstrates an accessible methodology for analyzing land use and land cover change at the urban and suburban scale using Sentinel-2 satellite imagery and NDVI classification programs. The tool democratizes remote sensing analysis for researchers across multiple disciplines by not requiring specialized software or large budgets. Through case studies of Warrenton, Virginia and Portland, Oregon, the method successfully detected contrasting patterns of vegetation change associated with different urban development approaches - suburban sprawl versus urban densification.

While the current version has limitations in spatial resolution and temporal coverage, the methodology provides a foundation that can be enhanced as newer datasets from more advanced sensors become publicly available. The statistical framework incorporating correlation and regression analysis adds rigor beyond simple visual study, allowing researchers to determine relationships between development and vegetation change. Future improvements through ground-truthing and enhanced satellite data could strengthen the applicability of this approach for urban planning, conservation, and environmental monitoring applications.

### Code and Data Availability

The web application is publicly accessible at: <https://terrestrialresearch.com/machinelearning/landclass2>

Source code is available at: <https://github.com/aurashak/ndvilandclass>

Data used in this study is freely available through the Copernicus Open Access Hub: <https://scihub.copernicus.eu/>

### Data and Software

Satellite imagery data were provided by the ESA via the Copernicus Open Access Hub. The author acknowledges the open source software communities that developed and maintain the Python libraries (NumPy, SciPy, Matplotlib, Pillow), JavaScript frameworks (Leaflet.js), and geospatial tools (QGIS) used in this research. Free and open source Large Language Models were used to assist with web development as described in Section 2.2.3.

|   |     |
|---|-----|
| <b>Abbreviations</b>  | 522 |
| API   | 524 |
| CHIME   | 525 |
| CSDA  | 526 |
| ESA   | 527 |
| GIS   | 528 |
| HTML  | 529 |
| LULCC   | 530 |
| MSI   | 531 |
| NASA  | 532 |
| NDVI  | 533 |
| NIR   | 534 |
| NLCD  | 535 |
| R <sup>2</sup>  | 536 |
| RGB   | 537 |
| SBG   | 538 |
| SWIR  | 539 |
| TOD   | 540 |
| UGB   | 541 |
| USGS  | 542 |
| VHR   | 543 |
|   | 544 |
| <b>Bibliography</b>   | 545 |
| 1. Agafonkin, V. (2011). Leaflet: An open-source JavaScript library for mobile-friendly interactive maps. Available at: <a href="https://leafletjs.com">https://leafletjs.com</a>   | 546 |
|   | 547 |
| 2. Abbott, C. (2001) <i>Greater Portland: Urban Life and Landscape in the Pacific Northwest</i> . Philadelphia: University of Pennsylvania Press.   | 548 |
|   | 549 |
| 3. Anderson, J.R., Hardy, E.E., Roach, J.T., & Witmer, R.E. (1976). A land use and land cover classification system for use with remote sensor data. USGS Professional Paper 964. Washington, DC: U.S. Geological Survey.   | 550 |
|   | 551 |
|   | 552 |
| <a href="https://pubs.usgs.gov/pp/0964/report.pdf">https://pubs.usgs.gov/pp/0964/report.pdf</a>   | 553 |
| 4. Drusch, M., Del Bello, U., Carlier, S., Colin, O., Fernandez, V., Gascon, F., ... & Bargellini, P. (2012). Sentinel-2: ESA's optical high-resolution mission for GMES operational services. <i>Remote Sensing of Environment</i> , 120, 25-36. <a href="https://www.sciencedirect.com/science/article/abs/pii/S0034425712000636">https://www.sciencedirect.com/science/article/abs/pii/S0034425712000636</a> | 554 |
|   | 555 |
|   | 556 |
|   | 557 |
| 5. EOportal (2025). <i>WorldView Legion Specifications</i> . <a href="https://www.eoportal.org/satellite-missions/worldview-legion">https://www.eoportal.org/satellite-missions/worldview-legion</a>  | 558 |
|   | 559 |
| 6. European Space Agency (2025). <i>S2 Mission - SentiWiki</i> . <a href="https://sentiwiki.copernicus.eu/web/s2-mission">https://sentiwiki.copernicus.eu/web/s2-mission</a>  | 560 |
|   | 561 |

7. ESA (European Space Agency). (2024). Sentinel-2C joins the Copernicus family in orbit. [https://www.esa.int/Applications/Observing\\_the\\_Earth/Copernicus/Sentinel-2/Sentinel-2C\\_joins\\_the\\_Copernicus\\_family\\_in\\_orbit](https://www.esa.int/Applications/Observing_the_Earth/Copernicus/Sentinel-2/Sentinel-2C_joins_the_Copernicus_family_in_orbit)
8. Google Earth (2025) Google Earth. <https://earth.google.com>
9. Goward, S.N., Markham, B., Dye, D.G., Dulaney, W., & Yang, J. (1991). Normalized difference vegetation index measurements from the Advanced Very High Resolution Radiometer. *Remote Sensing of Environment*, 35(2-3), 257-277. <https://www.sciencedirect.com/science/article/abs/pii/003442579190017Z>
10. Harris, C.R., Millman, K.J., van der Walt, S.J., Gommers, R., Virtanen, P., Cournapeau, D., ... & Oliphant, T.E. (2020). Array programming with NumPy. *Nature*, 585(7825), 357-362. <https://www.nature.com/articles/s41586-020-2649-2>
11. Homer, C., Dewitz, J., Jin, S., et al. (2020). Conterminous United States land cover change patterns 2001–2016 from the 2016 National Land Cover Database. *ISPRS Journal of Photogrammetry and Remote Sensing*, 162, 184-199. <https://www.sciencedirect.com/science/article/pii/S0924271620300587>
12. Hunter, J.D. (2007). Matplotlib: A 2D graphics environment. *Computing in Science & Engineering*, 9(3), 90-95. <https://ieeexplore.ieee.org/document/4160265>
13. Lunetta, R.S., Knight, J.F., Ediriwickrema, J., Lyon, J.G., & Worthy, L.D. (2006). Land-cover change detection using multi-temporal MODIS NDVI data. *Remote Sensing of Environment*, 105(2), 142-154. <https://www.sciencedirect.com/science/article/abs/pii/S0034425706002549>
14. Metro. (2023). Urban Growth Boundary. Portland Metro Regional Government. <https://www.oregonmetro.gov/what-metro-does/land-use-and-development/2040-growth-concept/urban-growth-boundary>
15. NASA Jet Propulsion Laboratory (2023) *Surface Biology and Geology (SBG)*. <https://sbg.jpl.nasa.gov/>
16. Pettorelli, N., Vik, J.O., Mysterud, A., Gaillard, J.M., Tucker, C.J., & Stenseth, N.C. (2005). Using the satellite-derived NDVI to assess ecological responses to environmental change. *Trends in Ecology & Evolution*, 20(9), 503-510.
17. Qwen Team. (2023). *Qwen Coder*. Available at: <https://github.com/QwenLM/Qwen-Coder> [accessed on: November 2023]
18. Romaniuk, Paweł & Saeed, Khalid & Boucetta, Rahma. (2023). *Exploring Object Size Estimation Through Low-Cost Drone Technology*. [https://www.researchgate.net/publication/371703546\\_Exploring\\_Object\\_Size\\_Estimation\\_Through\\_Low-Cost\\_Drone\\_Technology](https://www.researchgate.net/publication/371703546_Exploring_Object_Size_Estimation_Through_Low-Cost_Drone_Technology)
19. Singh, A. (1989). Digital change detection techniques using remotely-sensed data. *International Journal of Remote Sensing*, 10(6), 989-1003. <https://www.tandfonline.com/doi/abs/10.1080/01431168908903939>
20. Tucker, C.J. (1979). Red and photographic infrared linear combinations for monitoring vegetation. *Remote Sensing of Environment*, 8(2), 127-150. <https://www.sciencedirect.com/science/article/abs/pii/0034425779900130>

21. Verbesselt, J., Hyndman, R., Newnham, G., & Culvenor, D. (2010). Detecting trend and seasonal changes in satellite image time series. *Remote Sensing of Environment*, 114(1), 106-115. <https://www.sciencedirect.com/science/article/abs/pii/S003442570900265X>
22. VanderPlas, J. (2016). *Python Data Science Handbook: Essential Tools for Working with Data*. O'Reilly Media. <https://jakevdp.github.io/PythonDataScienceHandbook/>
23. Virtanen, P., Gommers, R., Oliphant, T.E., Haberland, M., Reddy, T., Cournapeau, D., ... & SciPy 1.0 Contributors. (2020). SciPy 1.0: fundamental algorithms for scientific computing in Python. *Nature Methods*, 17(3), 261-272. <https://www.nature.com/articles/s41592-019-0686-2>
24. Wilder, K. and Mackun, P. (2025). U.S. Metro Areas Experienced Population Growth Between 2023 and 2024. <https://www.census.gov/library/stories/2025/04/metro-area-trends.html>